Proceedings of the 12th International Conference on
Aluminium Alloys, September 5-9, 2010, Yokohama, Japan

pp. 1367-1372

Application of Electron Tomography for Characterizing Precipitate Morphologies in Aluninum Alloys

Kenji Kaneko
Department of Material Science and Engineering, Kyushu University
Room 650, West 4, 744, Motooka, Nishi, Fukuoka, 819-0395, Japan

Nanoscale characterization plays a vital role in both design and property of materials used in nanoscience and nanotechnology. To date, large numbers of journal papers have been published concerning microstructures and nanostructures of materials based on TEM images displaying 2D projected images, which is not reflecting the true 3D nature of the materials, but authors have to correlate 2D images with 3D physical properties. Recent development of fully-digitized and automated TEM as well as advancement of fast computers with combination of computed tomography let us achieve three-dimensional electron tomography (3D-ET). 3D-ET is a useful technique for reconstructing a 3D object from tilt series of 2D projections acquired by a TEM, for not only to determine the size and distribution of objects but also to provide information about the 3D morphology of them in the order of nanometer. In fact, 3D analyses provide very different types of information achieved by conventional 2D analyses, which are very essential in material science. In fact, it is extremely important to comprehend the correlation between the 3D physical properties of materials and their sizes, structures, compositions, distributions and morphologies.

Keywords: *Transmission Electron Microscopy, Electron Tomography, Alloys, Precipitates.*

1. Introduction

In general, physical and chemical properties of materials are dependent on their sizes, structures, compositions, morphologies and distributions. Transmission electron microscopy (TEM) has been an essential technique to characterize materials for a few decades, and playing an important role to understand 2D structures in the nano-order. Although TEM has advantages of observing the internal structures of the specimen, it has difficulties in observing the structural details from the different depths.

3D-ET, a technique established in the field of life sciences, has been developed for materials science very recently, which is a useful technique for reconstructing 3D objects from a tilt series of projections acquired by a transmission electron microscope (TEM) [1]. In addition, recent development of fully-digitized and automated TEM with combination of computed tomography let us achieve the 3D-ET, for not only to determine the size and distribution of objects but also to provide information about the 3D morphology of them in the order of nanometer. The specimen was usually tilted around a single axis at different angles, from -70^o to 70^o, to acquire a series of projections, since the beam direction cannot be changed in the TEM by a large amount, and the spatial resolution in all directions is about 1.0 nm [2]. 3D structure was then reconstructed by processing the series of 2D projections by combination of reconstruction and visualization software [3].

In this talk, (1) the morphological transformation of spherical precipitates due to severe plastic deformation, and (2) distribution and morphological information of precipitates, will be presented.

2. Specimens

2.1 Al-Ag alloy

High-purity (99.99%) Al and high-purity (99.9%) Ag were melted in air, cast into an ingot with dimensions of 17×55×120 mm^3, and then homogenized at 753 K for 24 h. Chemical analysis after homogenization showed the alloy contained 10.8 mass% Ag. The ingot was cut into bars with dimensions of 15×15×120 mm^3, swaged into rods with diameters of 10 mm, and then cut to lengths of ~60 mm for processing by equal-channel angular pressing (ECAP). Processing by ECAP was conducted at room temperature using a die having a channel angle Φ of 90^o and with an internal arc of curvature $\Psi \sim 20^o$ at the point of intersection of the two channels. It can be shown that these values of Φ and Ψ lead to an equivalent bulk strain of 1 on each passage through the die. Aging was conducted at temperatures of 200 ^{o}C for 10 h with the aging applied both to samples processed by ECAP and to samples subjected to the solution treatment but without ECAP.

2.2 Al-Ge alloy

Al-1.6at.% Ge was prepared from a melt of 99.99% purity Al and 99.999% purity Ge starting materials using an electric-arc furnace in an argon atmosphere. The specimen was then homogenized at 420 ^{o}C for 24 hours, and quenched in water to room temperature. Specimens for transmission electron microscopy were prepared by twin-jet electro-polishing with a solution of 40% acetic acid, 30% orthophosphoric acid, 20% nitric acid and 10% water at a temperature of 20 ^{o}C and 12V (0.2A).

2.3 Al-Si alloy

An Al–1.5 at% Si alloy was prepared from high-purity (99.99%) Al and high purity (99.9%) Si. The alloy was melted in air, cast into an ingot and then homogenized at 843K for 24 h. The ingot was solution treated at 850K for 1 h and aged at 473K for 5 h for the precipitation of Si-phases. For TEM studies, 3mm diameter samples were punched from thin slices with 0.3mm thickness and ground to approximately 0.1mm thickness. A Gatan Model 656 Dimple Grinder and a Model 691 Precision Ion Polishing System were used to produce thin TEM foils.

3. Experimental Method

3.1 TEM

Transmission electron microscopy (TEM) was performed on two different microscopes. Structures were examined by a BF-TEM (JEM-3200FSK, JEOL, Japan and TECNAI-F20, FEI, The Netherlands). 3D-ET observations with a scanning-TEM high-angle annular dark-field (STEM-HAADF) detector were conducted by computer-controlled fully-digitized TEM (TECNAI-20 and TECNAI-F20, FEI., Eindhoven, The Netherlands) with specially designed high-tilt holders (Model 2020 Advanced tomography holder, E. A. Fischione Instruments Inc., U.S.A.[4] and HATA holder, Melbuild, Japan [5]).

3.2 3D-ET

In the case of 3D-ET, many TEM parameters are controlled during the acquisition of the tilt series of projections: the defocus, the beam shift, the beam tilt, the image shift, the specimen tilt, and the specimen height. During the tilt series acquisition, it is also necessary to consider the increase of thickness with increase of tilt angle, e.g. the path length of the electron beam through the specimen becomes approximately three times at 70°. The quality of the reconstructed volume also decreases by the increase of the amount of inelastic scattering electron, due to the relative specimen thickness increase by tilting the specimen at higher degrees. For this case, energy-filtering method can be applied to acquire zero-loss image so that to improve the image quality. In addition, it is possible to acquire the reconstructed three-dimensional image from the plasmon-loss images and core-loss images. Furthermore, it is possible to reduce the effect of Bragg scattering by using high-angle annular dark-field imaging method to achieve final reconstructed images.

Depth resolution of 3D-ET method is in the order of a few nanometers, thus it is clearly possible to distinguish the nanoparticles which are separated for a few nanometers. The spatial resolution and the quality of reconstructed volume are strongly dependent on that of original image, on the angular range and on the angular increment. The smaller the tilt increment, the better quality can be achieved in the reconstruction. Furthermore, the total tilt range determines the amount of 3D data seen over all tilt angles. The larger the total tilt angle, the more qualitative data can be seen in the reconstruction.

Imaging from various tilt angles provides information of depth which enables distinction of overlapped structure. As can be seen in Fig. 1, even if the particles are observed as almost overlapping each other within the field of view from one direction, it can be seen separated from another direction.

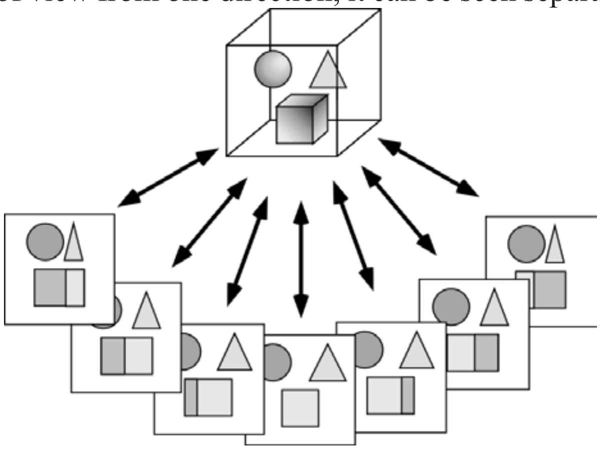

Fig. 1. A schematic diagram of acquiring 2D projections and achieving 3D reconstructed volume.

Data collection for TEM-CT is usually carried out by tilting the specimen around a single axis in the electron beam. In general, the spatial resolution of the reconstruction is anisotropic for the single-axis tilt geometry. In practice, the limited space between the objective lens pole pieces and the finite thickness of the specimen holder limits the tilt range, giving rise to the missing wedge of information, as schematically shown in Fig. 2.

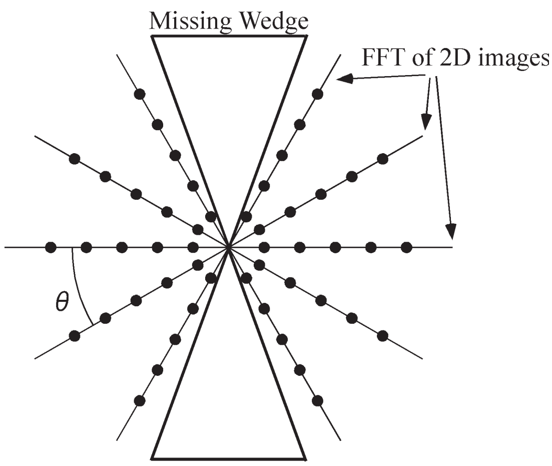

Fig. 2. Due to the absence of the images at higher tilt angle, as indicated missing wedge within the figure, so that it is difficult to achieve perfect three-dimensional reconstructed volume.

This missing information leads to the lowering resolution in the direction parallel to the optic axis by an ‘elongation factor’, e, by

$$e = \sqrt{\frac{\alpha_{\max} + \cos\alpha_{\max}\sin\alpha_{\max}}{\alpha_{\max} - \cos\alpha_{\max}\sin\alpha_{\max}}} \tag{1}$$

Recently, a specimen preparation method is proposed in the shape of cylindrical rod and rotates it for 360º to avoid missing edges [6]. Usually, supramolecules are supported on an amorphous carbon

TEM grid, so that it is necessary to consider the thickness of the amorphous film support, size, shape and structure of supramolecules to decide the tilt angles.

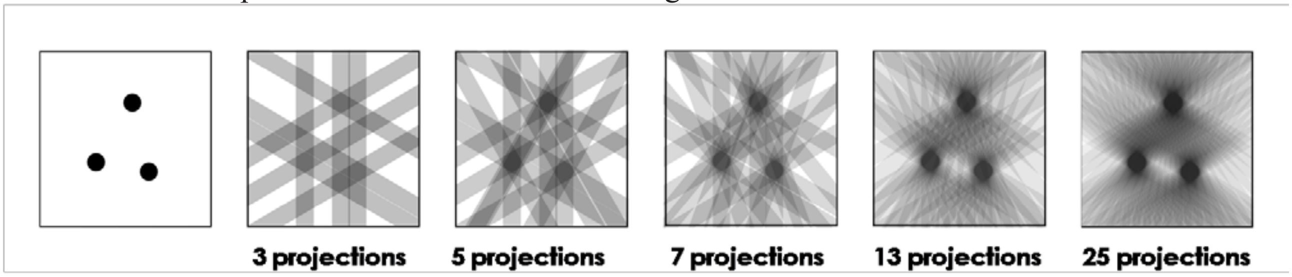

Fig. 3. The relationship between the number of projections and the tilt increments, with the same tilt range, from -60º to 60º.

The improvements of spatial resolution and the image quality of the reconstructed image require large numbers of tilted images and from high angles, see Fig. 3. This suggests that the total amount of time achieving tilted images requires the simple multiplication of the time taken to obtain one image and the number of images required, from the same field of view, which results the higher possibilities of the irradiation damage and the contamination over the field of view. Furthermore, large numbers of tilted images require large amount of processing time and memories.

In the present case, series of projections were acquired typically from -70° to 70°, with either BF-TEM or STEM-HAADF images recorded every 2° giving a total of 71 images. A HAADF detector collects electrons that undergo high-angle scattering and the signal is approximately proportional to Z^2, in which Z is the atomic number. It is therefore that the STEM-HAADF image is also known as Z-contrast image. In particular, Z-contrast imaging method is useful to study (poly-)crystalline materials because the coherent diffraction contrast can be minimized.

Once the acquisition of the tilt series is completed, the data is transferred to a PC for alignment and 3D reconstruction. Images were spatially aligned by a cross-correlation algorithm using Inspect3D software (FEI, Einthoven), and 3D reconstructions were achieved using a simultaneous iterative reconstruction technique (SIRT) of consecutive 2D slices. Visualization was performed using AVIZO Fire 6.1 (Visualization Sciences Group) [7].

4. Results

4.1 Al-Ag alloy [8]

Morphologies of GP zones and γ' phases in Al–Ag binary alloys, pre- and post-deformation by application of local strain were examined. Severe plastic deformation was applied to an Al–Ag alloy using the ECAP process, which enables a control over the amount of shear strain on the GP zones and γ' phases by moving dislocations. The formation of shear bands was easily recognized from both BF-TEM images and 3D-ET reconstructed volumes of GP zones, as spherical one from pre-deformed specimen and ellipsoidal one at the shear band from post-deformed specimen, as shown in Fig. 4.

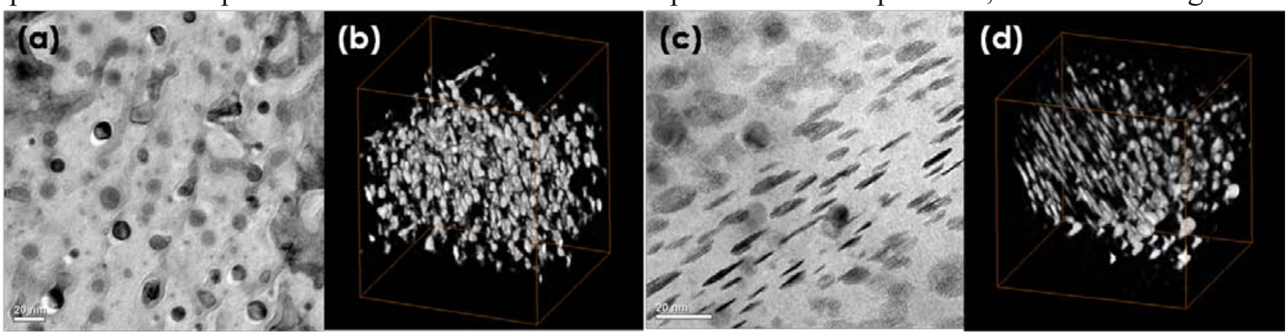

Fig. 4 (a) a BF image and (b) a reconstructed 3D volume of pre-deformed specimen and (c) a BF-image and (d) a reconstructed 3D volume of post-deformed specimen.

4.2 Al-Ge alloy [9]

Fig. 5 shows (a) a 2D STEM-HAADF image and (b) a reconstruction of Ge precipitates from almost the same field of view. A variety of Ge precipitates were clearly seen at different depths. In particular, precipitates judged as triangular shape in 2D image are judged as triangular-plate, tetrahedra and octahedrain 3D.

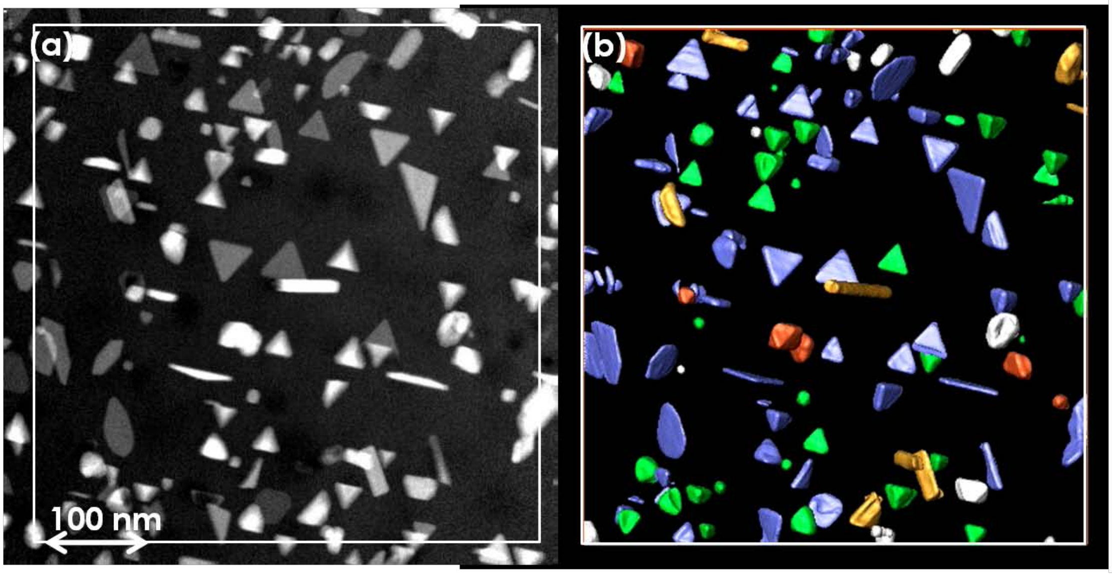

Fig. 5 (a) a STEM-HAADF image and (b) a reconstructed 3D volume from the same field of view.

4.3 Al-Si alloy [10]

In the case of the Al–Si system, the effect of mass and thickness contrast can be ignored from the cause of contrast in 2D. For example, the tilt series should be acquired from the region of the same thickness, and the atomic numbers of both Al (Z=13) and Si (Z=14) are almost the same. The diffraction contrast of plate-type and rod-type Si-phases with different diffraction characteristics from the matrix were applied to achieve BF-TEM images so that to reconstruct the 3D volumes, as shown in Fig. 6.

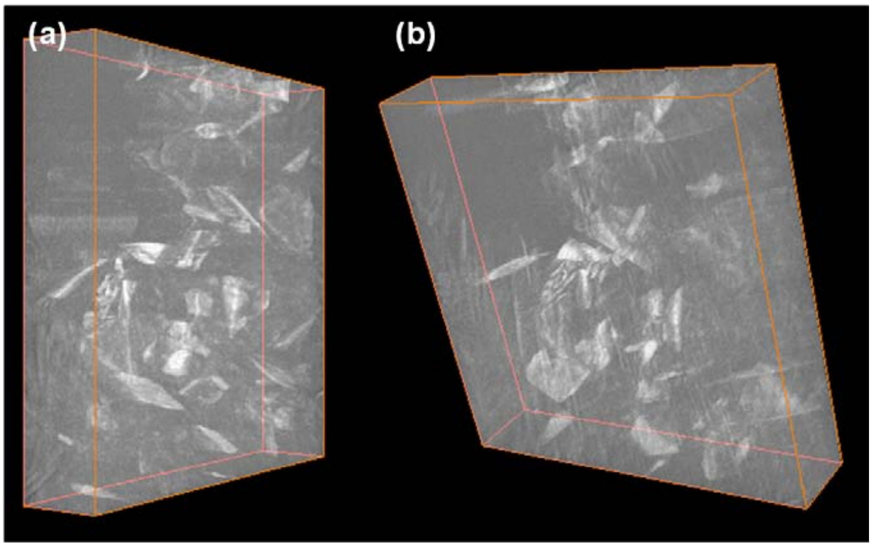

Fig. 6 Reconstructed volume-rendered images viewing from different orientation of a Si-phase showing a clear morphology of plate- and rod-type Si-phases.

5. Conclusion

The present study demonstrated three-dimensional morphologies of particles and precipitates at nanoscale in various materials. Nanoscale characterization plays a vital role in both the design and property of materials used in nanotechnology. So far, large numbers of papers have been published concerning nanoscale materials based on TEM images which display 2D projected images, which is not exactly reflecting the true 3D morphologies of the materials, and authors had to correlate those results with 3D physical properties of nanoscale materials. I would like to emphasize that both 2D information and 3D information are imperative to characterize 3D objects at nanoscale.

Acknowledgment. This work was supported in part by JST-CREST, “Grant-in-Aid for Scientific Research” and “Grant-in-Aid for the Global COE Program (Future Molecular Science)” of the Ministry of Education, Culture, Sports, Science and Technology of Japan.

References

[1] J. Frank: Academic Press, San Diego, 1996.
[2] P. A. Midgley, M. Weyland: Ultramicroscopy 96 (2003) 413–431.
[3] J. R. Kremer, D. N. Mastronarde, J. R. McIntosh: J Struct Bio 116 **(**1996**)** 71–76.
[4] http://www.fischione.com/products/model_2020.asp
[5] http://www.melbuild.com/newprouct_ST_EG_2.html
[6] N. Kawase, M. Kato, H. Nishioka, H. Jinnai: Ultramicroscopy 107 (2007) 8–15.
[7] http://www.vsg3d.com/vsg_prod_avizo_overview.php
[8] K. Inoke, K. Kaneko, M. Weyland, P. A. Midgley, K. Higashida, and Z. Horita: Acta Materialia 54 (2006) 2957–2963.
[9] K. Kaneko, K. Inoke, K. Sato, K. Kitawaki, H. Higashida, I. Arslan, P. A. Midgley: Ultramicroscopy 108 (2008) 210–220.
[10] K. Kaneko, R. Nagayama, K. Inoke, E. Noguchi, Z. Horita: Science and Technology of Advanced Materials 7 (2006) 726–731.